NASA/TM—2015-218408

Geometry and Simulation Results for a Gas Turbine Representative of the Energy Efficient Engine (EEE)

Russell W. Claus
Glenn Research Center, Cleveland, Ohio

Tim Beach
Coyote Hollow Consulting, LLC, Walton Hills, Ohio

Mark Turner and Kiran Siddappaji
University of Cincinnati, Cincinnati, Ohio

Eric S. Hendricks
Glenn Research Center, Cleveland, Ohio

February 2015

NASA STI Program . . . in Profile

Since its founding, NASA has been dedicated to the advancement of aeronautics and space science. The NASA Scientific and Technical Information (STI) Program plays a key part in helping NASA maintain this important role.

The NASA STI Program operates under the auspices of the Agency Chief Information Officer. It collects, organizes, provides for archiving, and disseminates NASA's STI. The NASA STI Program provides access to the NASA Technical Report Server—Registered (NTRS Reg) and NASA Technical Report Server—Public (NTRS) thus providing one of the largest collections of aeronautical and space science STI in the world. Results are published in both non-NASA channels and by NASA in the NASA STI Report Series, which includes the following report types:

- TECHNICAL PUBLICATION. Reports of completed research or a major significant phase of research that present the results of NASA programs and include extensive data or theoretical analysis. Includes compilations of significant scientific and technical data and information deemed to be of continuing reference value. NASA counter-part of peer-reviewed formal professional papers, but has less stringent limitations on manuscript length and extent of graphic presentations.

- TECHNICAL MEMORANDUM. Scientific and technical findings that are preliminary or of specialized interest, e.g., "quick-release" reports, working papers, and bibliographies that contain minimal annotation. Does not contain extensive analysis.

- CONTRACTOR REPORT. Scientific and technical findings by NASA-sponsored contractors and grantees.

- CONFERENCE PUBLICATION. Collected papers from scientific and technical conferences, symposia, seminars, or other meetings sponsored or co-sponsored by NASA.

- SPECIAL PUBLICATION. Scientific, technical, or historical information from NASA programs, projects, and missions, often concerned with subjects having substantial public interest.

- TECHNICAL TRANSLATION. English-language translations of foreign scientific and technical material pertinent to NASA's mission.

For more information about the NASA STI program, see the following:

- Access the NASA STI program home page at http://www.sti.nasa.gov

- E-mail your question to help@sti.nasa.gov

- Fax your question to the NASA STI Information Desk at 757-864-6500

- Telephone the NASA STI Information Desk at 757-864-9658

- Write to:
  NASA STI Program
  Mail Stop 148
  NASA Langley Research Center
  Hampton, VA 23681-2199

NASA/TM—2015-218408

Geometry and Simulation Results for a Gas Turbine Representative of the Energy Efficient Engine (EEE)

Russell W. Claus
Glenn Research Center, Cleveland, Ohio

Tim Beach
Coyote Hollow Consulting, LLC, Walton Hills, Ohio

Mark Turner and Kiran Siddappaji
University of Cincinnati, Cincinnati, Ohio

Eric S. Hendricks
Glenn Research Center, Cleveland, Ohio

National Aeronautics and
Space Administration

Glenn Research Center
Cleveland, Ohio 44135

February 2015

Acknowledgments

This research was supported by the Fixed-Wing element of the Fundamental Aeronautics Program at NASA. The authors would like to further acknowledge the assistance of Chris Miller, Bill Haller, Greg Follen, and Scott Townsend at NASA Glenn. This report would not be possible without the support of Andrew Breeze-Stringfellow and Pat Niskode (retired) at General Electric Airbreathing Engines.

This report is a formal draft or working paper, intended to solicit comments and ideas from a technical peer group.

This report contains preliminary findings, subject to revision as analysis proceeds.

This work was sponsored by the Fundamental Aeronautics Program at the NASA Glenn Research Center.

Level of Review: This material has been technically reviewed by technical management.

Available from

NASA STI Program
Mail Stop 148
NASA Langley Research Center
Hampton, VA 23681-2199

National Technical Information Service
5285 Port Royal Road
Springfield, VA 22161
703-605-6000

This report is available in electronic form at http://www.sti.nasa.gov/ and http://ntrs.nasa.gov/

Geometry and Simulation Results for a Gas Turbine Representative of the Energy Efficient Engine (EEE)

Russell W. Claus
National Aeronautics and Space Administration
Glenn Research Center
Cleveland, Ohio 44135

Tim Beach
Coyote Hollow Consulting, LLC
Walton Hills, Ohio 44146

Mark Turner and Kiran Siddappaji
University of Cincinnati
Cincinnati, Ohio 45220

Eric S. Hendricks
National Aeronautics and Space Administration
Glenn Research Center
Cleveland, Ohio 44135

Abstract

This paper describes the geometry and simulation results of a gas-turbine engine based on the original EEE engine developed in the 1980s. While the EEE engine was never in production, the technology developed during the program underpins many of the current generation of gas turbine engines. This geometry is being explored as a potential multi-stage turbomachinery test case that may be used to develop technology for virtual full-engine simulation. Simulation results were used to test the validity of each component geometry representation. Results are compared to a zero-dimensional engine model developed from experimental data. The geometry is captured in a series of Initial Graphical Exchange Specification (IGES) files and is available on a supplemental DVD to this report.

Nomenclature

BPR	By Pass Ratio
CAD	Computer Aided Design
EEE	Energy Efficient Engine
HPC	High Pressure Compressor
HPT	High Pressure Turbine
ICLS	Integrated Core Low Spool
IGES	Initial Graphical Exchange Specification
LPC	Low Pressure Compressor
LPT	Low Pressure Turbine
Nc	Corrected rotational speed
NLH	Non-Linear Harmonic
NPSS	Numerical Propulsion System Simulator

1.0 Introduction

NPSS (Numerical Propulsion System Simulator) was a NASA program created in the early 1990s to build a virtual engine simulation capability (Ref. 1). Leveraging advanced computing technologies, its

goal was to develop a framework that enabled reduced development timeframes based on virtual engine simulation. The project developed research efforts that explored multi-fidelity, multidiscipline models of engine systems to baseline computational accuracies and address fundamental questions exploring the practicality of the technique (Ref. 2). Today, NPSS is used as a zero-dimensional engine model simulation environment supporting the development of many new propulsion systems.

Beyond a few demonstrations (Refs. 2, 3, and 4) of full engine simulations, the practical application of NPSS remains as a zero-dimensional cycle model. Until recently, a full, three-dimensional simulation of a gas turbine engine was not a practical capability for any engineering organization. Today, many advances make full-engine simulations practical. First, computational resources for these simulations may be demanding but the advance of chip and software technology has greatly mitigated this challenge. Second, many engine component simulations employ proprietary codes and models which limit the utility of the simulation. Commercial codes, while not fully comprehensive, are making significant progress to reduce this limitation. A third limitation is the availability of geometry to test and improve component codes in a full system environment. Previous studies have used proprietary geometries that could not be further disseminated.

This report publishes geometry files from a series of reports (Refs. 5, 6, and 7) and the original Compter Aided Design (CAD) derived drawings. The geometry is captured in a series of Initial Graphical Exchange Specification (IGES) files. Some of these IGES files trace to the original CAD drawings for the EEE turbomachinery. Some of the files (specifically for the HPC) were not created from the original CAD drawings, but were recreated from the data in the NASA contractor report (Ref. 5). The original CAD-based files were used in a series of simulations by Hall (Ref. 4, 8, and 9).

A series of three-dimensional numerical simulations were conducted to validate the geometry. The High Pressure Compressor (HPC) was the most challenging component to simulate and the geometry from the two different sources provided significantly different results. A recommendation for component simulations is provided based on the calculations for each turbomachinery component of the engine. It is shown that these results, which should be considered preliminary, may be adequate to assemble into a full gas-turbine simulation. Additionally, it is hoped that the geometries can be used as multi-stage benchmark testcases to further the development of new models and simulation techniques.

2.0 EEE Geometry

In the 1980s, NASA funded the Energy Efficient Engine program to demonstrate fuel efficient designs for the next generation of transport aircraft. New low-emission combustor designs were tested to meet emissions goals. For the turbomachinery, the primary focus was to meet a 12 percent reduction in installed specific fuel consumption. Both Pratt & Whitney and General Electric (GE) were awarded development contracts. The GE design was carried forward into Integrated Core/Low Spool (ICLS) testing (Ref. 10). This full-system, integrated testing provides a full-engine dataset that was not available with the Pratt and Whitney design. The GE version was therefore selected for this study. Figure 1 illustrates the GE EEE design.

At the start of the NPSS program, one of the goals was to create a geometry database that could be freely distributed to participating stake-holders. A team of NASA engineers and contractors worked with the original CAD files (obtained from GE) and created a series of IGES surfaces representing the flow path and blade shapes for the EEE turbomachinery. These geometry files were used in a series of engine component and full system calculations by Hall (Ref. 4).

The overall EEE turbomachinery geometry, is illustrated in Figure 2. This figure displays the various engine components and indicates that each blade shape is represented by a series of cross-sectional views. The fan is captured by approximately 20 cross-sections, while the LPT displays only 5 cross-sections. These cross-sections are stacked radially and the turning between each cross-section can be fairly large, as is seen in Figure 3. IGES surfaces were constructed to closely match the cross-sections, but the significant variation between cross-sections made a perfect fit challenging. The variation between the cross-sections and the IGES surface may be a source of potential error in the blade shape representations.

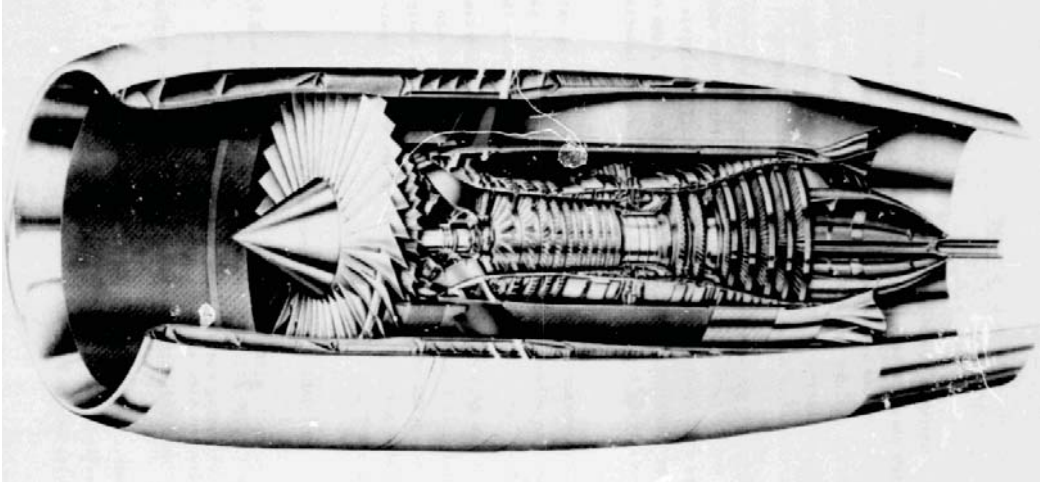

Figure 1.—Energy Efficient Engine developed by General Electric.

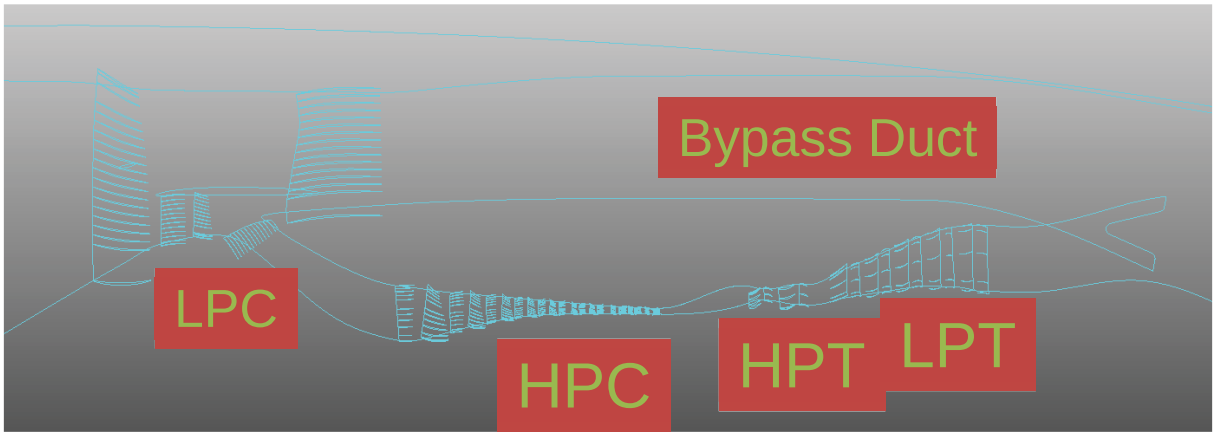

Figure 2.—Engine component geometry illustrated as a series of blade cross-sections.

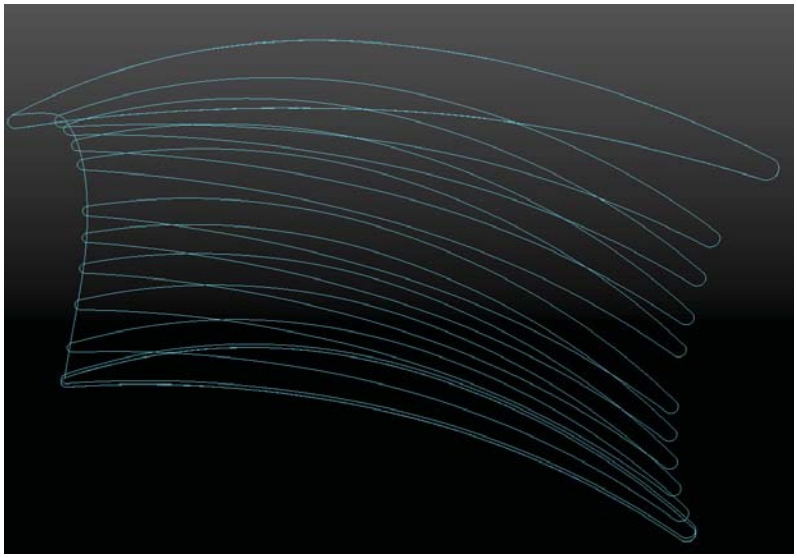

Figure 3.—Three-dimensional, perspective view of a stator blade showing the cross-sectional stacking and the radial shape variation.

Geometry files published with this report are organized as listed in Appendix A. Each component series of blade shapes is organized into a separate directory such as HPC, HPT, LPT or LPC. End walls or the limits of the flow domain can be extracted from the overall geometry file: "EEE_engine_all.igs" or "hub and casing" curves are provided in each component subdirectory. Blade counts are captured in Appendix B. In ensemble, these files provide much of the basic information needed for turbomachinery simulation. Information of the film-cooling or bleed can be extracted from Holloway (Ref. 6), Timko (Ref. 7) and Bridgeman (Ref. 11).

At the top directory, the "EEE_engine_all.igs" file is stored along with symmetric and unsymmetrical elements. The original tar file used to store all this data is also stored in the root directory. This original tar file stored the file information in a version-control application that mangled these file labels. However, for this publication, the file names have been repaired based on information contained within each IGES file.

The quarter stage booster and fan are included in the LPC directory. A series of curves provide information on the splitter and part-span shroud.

Two directories for the HPC can be seen. The first labeled "HPC" is derived from the same source as all the other geometry files (GE). The directory labeled "HPC-CR16558 Derived" was developed by Turner and Siddappaji at the University of Cincinnati, using only information in Holloway (Ref. 6). This reference noted that a variety of blade shapes were used in the HPC (NACA series, Circular Arcs and others), but it was unclear which blade shape was used for any particular rotor or stator. For this reason, the blade thickness was determined from a general area rule. These blade shapes display significant differences between the GE original CAD shapes and the IGES representations from Holloway (Ref. 6). Appendix C illustrates the difference in leading and trailing edge profiles between the two different series of files. Large discrepancies are seen in the rotors 8, 9 and 10 and several stators.

The EEE HPC was developed in the 1980s with two different "builds" or test articles. The second build was developed to improve on the original geometry documented in Holloway (Ref. 6). Holloway represents the first build while the geometry GE CAD shapes represent the second build. The impact of this variation will be discussed in Section 3.0, Engine System Performance.

HPT and LPT directories are organized as the other components.

2.1 Open Data Sources for the EEE Geometry

As has been noted in the previous section, the blade shapes for each component of the EEE can be largely reconstructed from the NASA Contractor Reports (Refs. 6, 7, 10, and 11). HPC shapes were extracted from Holloway (Ref. 6) for the first build of the EEE HPC. HPT blade coordinates were listed in Appendix A of Timko (Ref. 7). Scale drawings of the blade cross-section at three radial locations (hub, pitch and tip) are also available in this reference. Figure 1 in Timko provided detailed dimensions for the flow path. The LPT blade shapes were documented in Bridgeman (Ref. 11) through scale drawings of Figures 10 to 19. The flow path was documented in Figure 9. While these sources are not as reliable as the actual CAD representations, they do provide adequate information to analyze highly similar systems.

3.0 Engine System Performance

This section explores some numerical simulations of the EEE turbomachinery geometry documented in Section 2.0. New simulation results are placed in context by comparing with previous efforts (Ref. 4). Previous efforts were based on computer simulation technology of the 1990s with relatively course mesh resolution, constant gamma and a mixing plane treatment of the rotor / stator interaction. Modern CFD tools provide more options for numerical accuracy, much finer mesh resolution, and an improved treatment of the rotor / stator interaction using a Non-Linear Harmonic (NLH) method (Ref. 12). It was of interest to see if these improvements resulted in better system performance.

Numerical simulations of the rotating turbomachinery involved solving the Reynolds's Averaged Navier-Stokes equations using the Numeca FINE/Turbo code suite (Ref. 12). This software has a fully

integrated suite of tools that enables rapid mesh generation, domain decomposition, flow solving, and visualization. The mesh generation can be controlled through a series of utilities that tailor the grid topology and optimization to the application-specific geometry. Typically, the defaults for the mesh generation provide good mesh characteristics; however, adjustments were made using available manual controls. FINE/Turbo employs a variety of possible rotor/stator interface techniques, turbulence models, and differencing techniques. In this study, the steady-state options were used, including the Mixing Plane approximation, the Spalart-Almos turbulence model, and Flux Difference Splitting (second order upwind) with Min Mod limiters. Some calculations of the HPC were made using the NLH method.

Hall's simulation results (Ref. 4) (representative of early modeling efforts) can be seen in Table 1 for the simulated EEE system values and a cycle model. This cycle model was matched to the experimental engine tests(Ref. 10) by Owen and documented in Hall (Ref. 4). As can be seen in Table 1, the turbines exhibit poor corrected mass flow, pressure ratios, and efficiencies. However, the HPC is very well matched and the other compression components are all within a few percent of the cycle model results. Given the state of mesh resolution, constant gamma and model complexity in this study, the overall predictive accuracy is surprisingly good. However, if all these component simulations were fully coupled to the 0–D NPSS model, it seems likely that the predicted engine performance would not closely resemble the EEE.

With the recent advances in simulation capabilities, many of the EEE engine turbomachinery components have been analyzed again to better predict performance. Table 2 illustrates the component performance calculated using Fine/Turbo in these simulations for much of the EEE engine turbomachinery. The Fan/LPC component is not displayed as calculations of this component were not performed. Overall, the efficiency of each component is fairly good, with the exception of the LPT. The LPT displays a –3 percent performance variance. This level of inaccuracy may be due to a large number of factors, including poor development of the geometry, and model/mesh limitations. The good agreement seen in the HPT may be fortuitous as film cooling was not included and would likely alter the indicated performance.

All calculations were performed with smooth hub and casing surfaces, whereas, a more realistic representation would include hub leakages, turbine blade film cooling, secondary flow paths, and a capturing of the "button" geometry for the variable angle stators in the HPC. These calculations employed a mixing plane assumption for the rotor / stator interaction plane and better models may have improved the calculated results. The following sections discuss details of each component simulation.

TABLE 1.—ENGINE SYSTEM PERFORMANCE RESULTS OF HALL'S SIMULATIONS COMPARED WITH A 0–D CYCLE MODEL BASELINED TO EXPERIMENTAL DATA

	Wc, %	PR, %	Efficiency, %
FAN	3.23	–1.80	1.16
LPC	0.59	–1.67	1.99
HPC	–0.29	–0.22	–0.30
HPT	–6.17	–6.11	–2.88
LPT	10.11	11.49	–1.32

TABLE 2.—COMPONENT SIMULATION VARIANCES FROM THE BASELINE 0–D NPSS MODEL

Component	W, %	PR, %	Efficiency, %
HPC	3.45	–0.68	–0.89
HPT	6.64	1.55	0.32
LPT	8.32	2.32	–3.00

3.1 High Pressure Compressor (HPC)

The HPC was the most difficult component to simulate as might be expected from the high pressure-ratio compression performed by the system. The HPC, nominally, could perform at a pressure ratio of 25 although the calculations performed here were limited to about 23. As was reported earlier, the blade shapes directly traceable to GE CAD drawings had significant differences from the shapes developed from Holloway (Ref. 6). All calculations performed using the GE CAD geometry did not converge. The calculations reported here used the shapes derived from Holloway (Ref. 6).

Tip clearances were illustrated in Holloway (Ref. 6). Figure 4 is recreated from Figure 62 of this reference. The estimated line was presumably calculated using measured temperatures and pressure from rig testing. Two probe tip-clearance measurement locations were documented and match well within the estimated range of value.

The baseline HPC calculation seen in Table 2 was performed using the mixing plane assumption with flux-difference splitting of the momentum equations. The use of flux-difference splitting was important as central differencing resulted in reduced efficiencies and ultimately, the central difference calculation would not converge. The flux-differencing splitting, combined with mixing-plane, resulted in the work loading seen in Figure 5. This figure illustrates the percent of the total temperature rise occurring across each stage. The first two stages are highly loaded with the remaining stages experiencing between 9 and 10 percent temperature rise.

All HPC calculations were performed using 15,462,827 mesh nodes, with rotor blades typically employing about 1 million nodes and the stators at a lower level of resolutions of about 600K nodes.

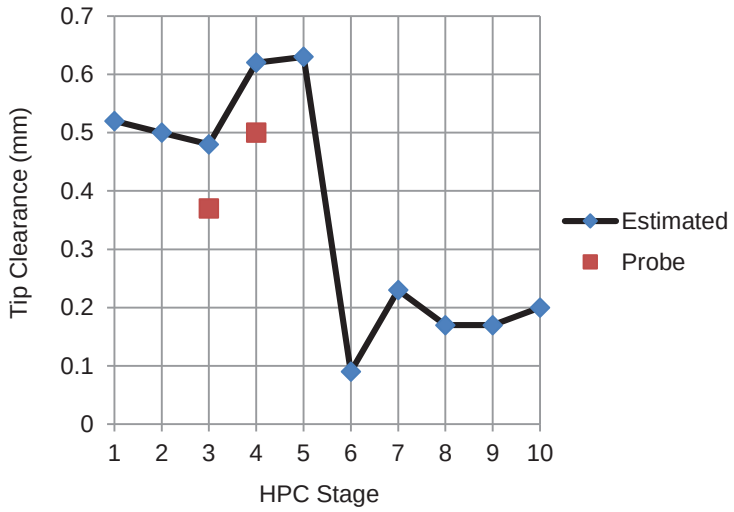

Figure 4.—HPC tip clearances as estimated and measured from Holloway.

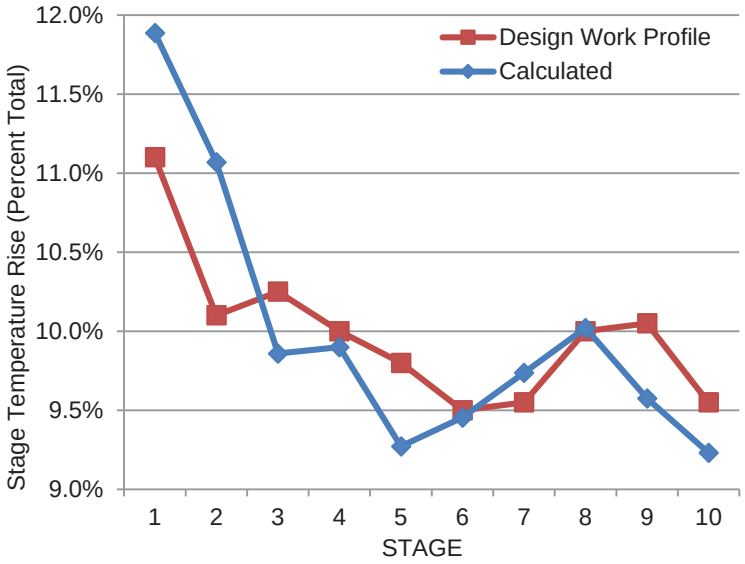

Figure 5.—Stage distribution of temperature rise (work loading) for the design and numerically calculated results.

3.2 High Pressure Turbine (HPT)

The HPT calculations were performed using Fine-Turbo with 3,828,020 nodes, central differencing, and with the mixing plane model for rotor / stator interactions. This simulation employed smooth sidewalls and no cooling bleed. The cooling bleed and sidewall treatment are obvious areas for improvement in this calculation. Despite these limitations the system performance is well predicted.

Nominal tip clearance was documented by Timko (Ref. 7) as 41 mm.

From Hall (Ref. 4): “GE engineers familiar with the actual test rig and EEE engine geometry recommended a one degree (open) reset of the LP turbine first stage vane.” This reset is maintained in these calculations.

3.3 Low Pressure Turbine (LPT)

The LPT calculation was performed with 12,410,092 nodes, central differencing and the mixing plane model. The calculated efficiency of 89.7 percent is lower that the cycle results, but this value is reasonable considering the limitations on the calculation. The boundary layer transition may be an area requiring further study / variation and, as with the HPT, bleed and sidewalls need to be improved. In general, the computed results are promising, but further study is suggested.

3.4 Summary

Overall, the component performance results suggest that a full coupling of the high-fidelity simulations with a 0D cycle simulation may be possible. Most component results are a fair match with system data. Much more simulation testing would be required to quantify the level of uncertainty, but the geometry provided by this report is certainly a good starting point for further refinement of the geometry and analysis features.

MN	alt	dTamb	W	Fg	Fn	SFC	Fuel	WAR	OPR
0.800	35000.0	18.00	524.5	21262.2	8351.3	0.5366	4480.99	0.0000	36.279

INPUT FLOW

	Tt	Pt	Ps	W	Wc	MN	Aphy	ht	Ts	FAR	gamt
Input_StrmTube >	464.50	5.292	3.458	522.12	1372.12	0.8000	4170.2	111.19	411.85	0.0000	1.40010
Input_EngInl >	464.50	5.292	3.860	522.12	1372.12	0.6868	4416.9	111.19	424.49	0.0000	1.40010
Input_FanSplit >	464.50	5.292	4.115	522.12	1372.12	0.6105	4703.7	111.19	432.29	0.0000	1.40010
Input_FanTip >	464.50	5.292	4.110	404.29	1062.47	0.6105	3646.5	111.19	432.29	0.0000	1.40010
Input_FanTipExtD>	543.01	8.625	7.524	404.29	704.82	0.4460	2996.3	130.03	522.25	0.0000	1.39973
Input_LPC >	464.50	5.292	4.110	117.83	309.65	0.6105	1062.7	111.19	432.29	0.0000	1.40010
Input_LPCSplit >	544.51	8.746	7.449	117.83	202.85	0.4844	810.5	130.38	520.11	0.0000	1.39973
Input_LPCTipDct >	544.51	8.746	7.439	53.83	92.68	0.4844	370.8	130.38	520.12	0.0000	1.39973
Input_LPCMix_I1 >	543.01	8.625	7.425	404.29	704.82	0.4676	2890.6	130.03	520.28	0.0000	1.39973
Input_LPCMix_I2 >	544.51	8.746	7.425	53.83	92.68	0.4893	367.6	130.38	519.64	0.0000	1.39973
Input_BypDct >	543.19	8.639	7.426	458.12	797.52	0.4700	3258.2	130.07	520.22	0.0000	1.39973
Input_BypBld >	543.19	8.278	0.000	458.12	832.31	0.0000	0.0	130.07	0.00	0.0000	1.39973
Input_HPCInlDct >	544.51	8.746	8.451	63.99	110.17	0.2220	862.1	130.38	539.20	0.0000	1.39973
Input_HPCInlBld >	544.51	8.746	7.774	63.99	110.17	0.4138	496.8	130.38	526.49	0.0000	1.39973
Input_HPC >	544.51	8.746	7.774	63.99	110.17	0.4138	496.8	130.38	526.49	0.0000	1.39973
Input_HPCExtBld >	1431.19	191.987	183.597	61.85	7.86	0.2576	54.4	351.36	1414.53	0.0000	1.35446
Input_Brn >	1431.19	191.987	185.751	53.66	6.82	0.2213	54.4	351.36	1418.87	0.0000	1.35446
Input_HPTInlBld >	2852.78	182.387	0.000	54.91	10.38	0.0000	0.0	774.14	0.00	0.0232	1.28458
HPT1Rcool >	1431.19	36.881	0.000	3.41	2.26	0.0000	0.0	351.36	0.00	0.0000	1.35446
HPT2Vcool >	1174.30	36.881	0.000	1.25	0.75	0.0000	0.0	285.07	0.00	0.0000	1.37012
Input_HPT >	2749.02	182.387	0.000	59.68	11.07	0.0000	0.0	740.33	0.00	0.0213	1.28883
Input_LPTInlBld >	1919.47	36.881	0.000	64.34	49.32	0.0000	0.0	493.87	0.00	0.0197	1.31737
Input_LPT >	1911.97	36.881	0.000	64.92	49.67	0.0000	0.0	491.64	0.00	0.0195	1.31778
Input_LPTExtDct >	1361.87	8.228	7.660	64.92	187.91	0.3274	1050.7	339.50	1337.08	0.0195	1.34503
Input_MainMix_I1>	543.19	8.278	7.016	458.12	832.31	0.4919	3288.4	130.07	518.13	0.0000	1.39973
Input_MainMix_I2>	1361.87	8.228	7.016	64.92	187.91	0.4913	755.4	339.50	1307.14	0.0195	1.34503
Input_Nozz >	650.48	8.211	6.881	523.05	1048.38	0.5094	4043.8	156.06	618.64	0.0024	1.39636
Input_NozzSnk >	650.48	8.211	4.345	523.05	1048.38	1.0000	3053.3	156.06	542.53	0.0024	1.39636
LPTcoolOB >	1013.95	61.699	0.000	0.31	0.10	0.0000	0.0	244.74	0.00	0.0000	1.38003
OvrBrd >	1013.95	61.699	0.000	0.31	0.10	0.0000	0.0	244.74	0.00	0.0000	1.38003

INLETS

	eRam	Afs	Fram
StrmTube	1.0000	4170.24	12910.9

DUCTS

	dPqP	MNin	Aphy
EngInl	0.00000	0.6868	4416.90
FanTipExt>	0.00000	0.4460	2996.30
LPCTipDct	0.00000	0.4844	370.82
BypDct	0.04180	0.4700	3258.19
HPCInlDct	0.00000	0.2220	862.10
LPTExtDct	0.00000	0.3274	1050.70

SPLITTERS

	BPR	dP/P1	dP/P2
FanSplit	3.43125	0.0000	0.0000
LPCSplit	0.84122	0.0000	0.0000

MIXERS

	%mix	MN1	MN2	A1	A2	Ps1	Ps2
LPCMix	1.00	0.468	0.489	2890.6	367.6	7.425	7.425
MainMix	1.00	0.492	0.491	3288.4	755.4	7.016	7.016

SHAFTS

	Nmech	trqIn	trqNet	pwrIn	HPX	dNqdt
LPShaft	3397.8	21601.3	-0.0058	13974.9	0.00	-0.00
HPShaft	12384.1	8378.1	0.0026	19755.0	0.00	0.00

COMPRESSORS & TURBINES

	Wc	PR	TR	efPoly	eff	Nc|Np	pwr
FanTip	1062.47	1.630	1.1690	0.8994	0.8936	3590.503	-10774.9
LPC	309.65	1.653	1.1722	0.9089	0.9033	3590.503	-3200.0
HPC	110.17	21.951	2.6284	0.8865	0.8332	12086.703	-19755.0
HPT	11.07	4.945	1.4024	0.9128	0.9270	236.2	19755.0
LPT	49.67	4.483	1.4039	0.9100	0.9247	77.7	13974.9

MAP POINTS - COMPRESSORS & TURBINES

	WcMap	PRmap	effMap	NcMap	R||parm
FanTip	1308.18	1.737	0.8397	99.726	2.0536
LPC	254.94	1.689	0.8644	99.726	1.6079
HPC	112.29	30.923	0.8013	100.208	1.1177
HPT	15.77	4.799	0.9213	99.137	76.0000
LPT	15.78	4.732	0.9210	98.394	76.0000

ADDERS AND SCALARS

	s_WcAud	a_WcAud			s_effAud	a_effAud
FanTip	1.0000	0.0000			1.0000	0.0000
LPC	1.0000	0.0000			1.0000	0.0000
HPC	1.0000	0.0000			1.0000	0.0000
	s_WpAud	a_WpAud	s_PRaud	a_PRaud	s_effAud	a_effAud
HPT	1.0000	0.0000	1.0000	0.0000	1.0000	0.0000
LPT	1.0000	0.0000	1.0000	0.0000	1.0000	0.0000

BLEEDS

		Wb/Win	dhb/dh	dPb/dP	Tt	ht
HPT2Vcool	HPC.HPT2Vcool	0.0195	0.7000	0.4953	1174.30	285.07
LPTcool	HPC.LPTcool	0.0091	0.5175	0.2890	1013.95	244.74

Figure 6.—Typical EEE engine system model output at cruise conditions.

4.0 EEE Engine Cycle

A 0–D representation of the ICLS engine was developed to support the simulations of Hall (Ref. 4). A typical output for cruise is illustrated in Figure 6. The complete NPSS model is included in accompanying compact disk. This model may be helpful to future efforts building a fully-coupled engine simulation.

5.0 Summary

The intent of this paper was to document the EEE geometry that may provide a baseline for testing full-engine simulation techniques. It appears highly likely that some of the geometry provided here may not be an exact representation of the hot, operating geometry for all components. The blade shapes received from GE did not contain blade surfaces, and the NURBS representations created for the blades may have flaws. Simulation results indicate reasonable component performance, but the accuracy is still subject to a variety of uncertainties. There is a great need to add detailed hub leakages models, variable stator “button” geometries, film cooling and end wall flows. The openly published contractor reports provide much of the information needed to further refine this geometry. The refined simulations might result in significantly different performance.

Appendix A.—Supplemental Information

Table 3 provides a listing of the files contained on the supplemental DVD available with this report.

TABLE 3.—LISTING OF FILES BY FOLDER CONTAINED IN SUPPLEMENTAL DVD

File Name	Date Modified	Size (bytes)
Directory: \EEE		
assem.igs	12/12/2012	28,436,480
directory.txt	12/19/2012	0
eee.tar.gz	12/12/2012	14,202,965
EEE_3d_sym.igs	12/12/2012	426,465
EEE_3d_uns.igs	12/12/2012	9,596,232
EEE_engine_all.igs	12/12/2012	8,736,255
HPC (Folder)	12/19/2012	
HPC-CR16558 Derived (Folder)	12/19/2012	
HPT (Folder)	12/19/2012	
LPC (Folder)	12/19/2012	
LPT (Folder)	12/19/2012	
Directory: \EEE\HPC		
case.igs	11/30/2009	41,310
compr_igv.igs	12/12/2012	194,319
compr_rotor1.igs	12/12/2012	275,400
compr_rotor10.igs	12/12/2012	187,353
compr_rotor2.igs	12/12/2012	275,886
compr_rotor3.igs	12/12/2012	249,804
compr_rotor4.igs	12/12/2012	241,380
compr_rotor5.igs	12/12/2012	241,461
compr_rotor6.igs	12/12/2012	219,510
compr_rotor7.igs	12/13/2012	222,426
compr_rotor8.igs	12/12/2012	217,161
compr_rotor9.igs	12/12/2012	195,048
compr_stator1.igs	12/12/2012	196,506
compr_stator10.igs	12/12/2012	171,477
compr_stator2.igs	12/12/2012	184,032
compr_stator3.igs	12/12/2012	146,448
compr_stator4.igs	12/12/2012	139,806
compr_stator5.igs	12/12/2012	118,422
compr_stator6.igs	12/12/2012	107,730
compr_stator7.igs	12/12/2012	119,637
compr_stator8.igs	12/12/2012	166,698
compr_stator9.igs	12/12/2012	148,716
hub.igs	11/30/2009	41,310
Directory: \EEE\HPC-CR16558 Derived		
blade1.igs	12/6/2011	376,083
blade10_cf.igs	2/24/2012	311,928
blade11_cf.igs	2/24/2012	308,730
blade12.igs	12/6/2011	376,083
blade13_cf.igs	2/24/2012	304,958
blade14.igs	12/6/2011	376,083
blade15.igs	12/6/2011	376,083
blade16.igs	12/6/2011	376,083
blade17.igs	12/6/2011	376,083
blade18_cf.igs	3/23/2012	306,352
blade19_cf.igs	4/4/2012	312,256

TABLE 3.—LISTING OF FILES BY FOLDER CONTAINED IN SUPPLEMENTAL DVD

File Name	Date Modified	Size (bytes)
blade2.igs	12/6/2011	376,083
blade20_cf.igs	4/4/2012	308,402
blade21_cf.igs	4/4/2012	311,354
blade3.igs	12/6/2011	343,845
blade4.igs	12/6/2011	376,083
blade5_cf.igs	2/24/2012	306,844
blade6.igs	12/6/2011	376,083
blade7.igs	12/6/2011	376,083
blade8.igs	12/6/2011	376,083
blade9.igs	12/6/2011	376,083
case.igs	11/30/2009	41,310
hub.igs	11/30/2009	41,310
README.txt	12/19/2012	593
Directory: \EEE\HPT		
case.igs	3/17/2010	21,402
hpt_rotor1.igs	12/12/2012	118,422
hpt_rotor2.igs	12/12/2012	113,967
hpt_stator1.igs	12/12/2012	116,640
hpt_stator2.igs	12/12/2012	107,568
hub.igs	3/17/2010	21,402
Directory: \EEE\LPC		
booster_rtr.igs	12/12/2012	270,135
booster_stator.igs	12/12/2012	607,338
Bypass_Outer.igs	3/23/2010	34,932
bypass_stator.igs	12/12/2012	644,112
core_guide_vane.igs	12/12/2012	402,327
fan.igs	12/14/2012	944,541
hub.igs	3/16/2010	22,468
LPC_bypass_hub.igs	3/25/2010	14,094
part_span_shroud_lower.igs	3/16/2010	6,068
part_span_shroud_upper.igs	3/16/2010	6,068
splitter_lower.igs	3/16/2010	21,238
splitter_upper.igs	3/16/2010	21,238
Directory: \EEE\LPT		
case.igs	3/17/2010	50,102
hub.igs	3/17/2010	50,102
lpt_rotor1.igs	12/12/2012	104,490
lpt_rotor2.igs	12/12/2012	103,761
lpt_rotor3.igs	12/12/2012	101,736
lpt_rotor4.igs	12/12/2012	103,923
lpt_rotor5.igs	12/12/2012	103,923
lpt_stator1.igs	12/12/2012	98,253
lpt_stator2.igs	12/12/2012	100,926
lpt_stator3.igs	12/12/2012	99,954
lpt_stator4.igs	12/14/2012	97,848
lpt_stator5.igs	12/12/2012	94,932

Appendix B

Table 4 lists circumferential blade counts for the various turbomachinery components of the EEE.

TABLE 4.—CIRCUMFRENTIAL BLADE COUNT FOR EACH BLADE ROW

LPC Blade	Count		HPC Blade	Count	HPT Blade	Count	LPT Blade	Count
1	32		1	32	1	46	1	72
2	60		2	28	2	76	2	120
3	56		3	50	3	48	3	102
4	64		4	38	4	70	4	122
5	34		5	50			5	96
			6	68			6	122
			7	82			7	114
			8	60			8	156
			9	92			9	120
			10	70			10	110
			11	110				
			12	80				
			13	120				
			14	82				
			15	112				
			16	84				
			17	104				
			18	88				
			19	118				
			20	96				
			21	140				

Appendix C

Figure 7 to Figure 28 document the difference between geometry-specified leading and trailing edges for all blades of the HPC. The blades labeled UC were developed by Turner and Kiran. The Allison shapes trace back to the original CAD drawings.

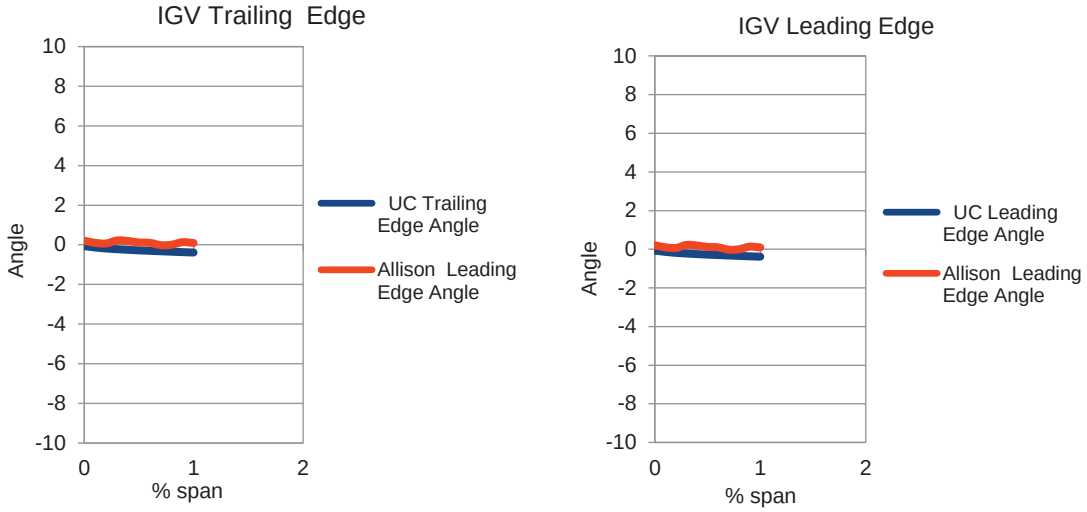

Figure 7.—Comparison of the trailing and leading edge of the IGV.

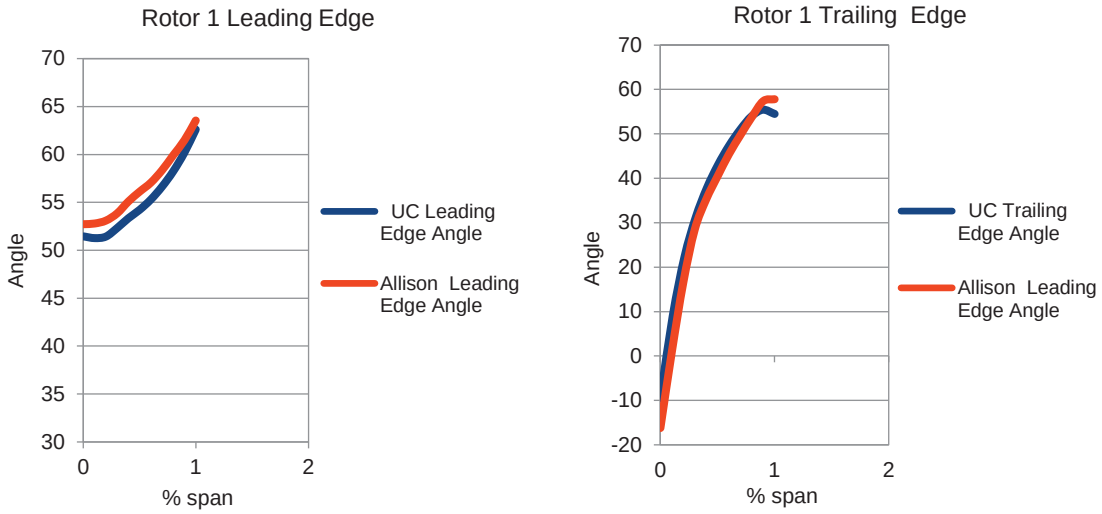

Figure 8.—Comparison of the trailing and leading edge of Rotor 1.

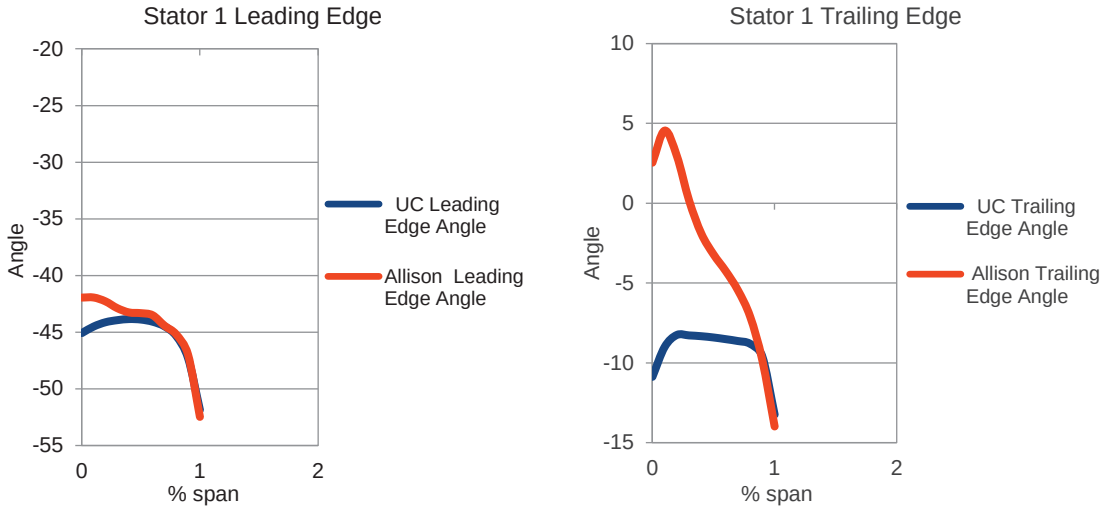

Figure 9.—Comparison of the trailing and leading edge of Stator 1.

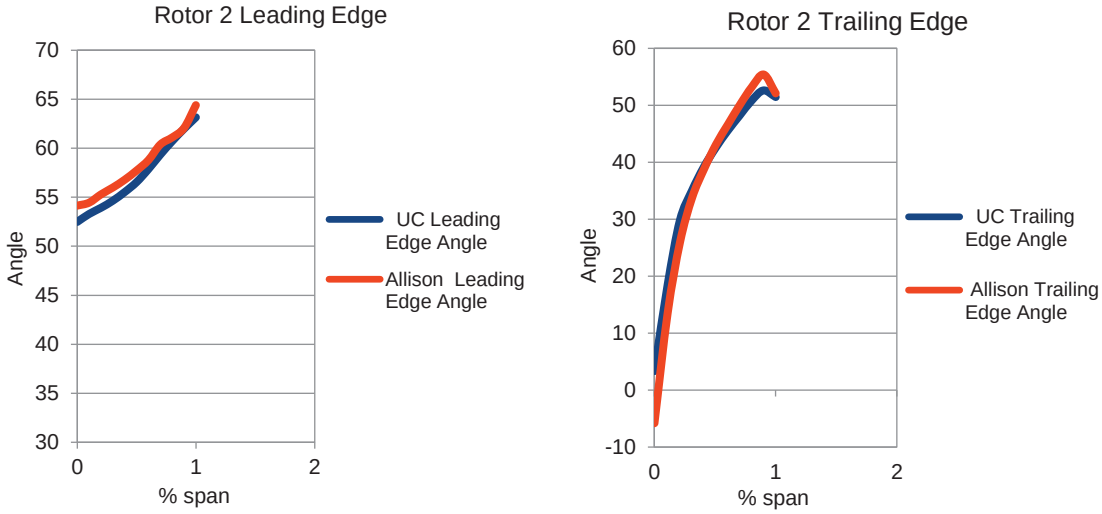

Figure 10.—Comparison of the trailing and leading edge of Rotor 2.

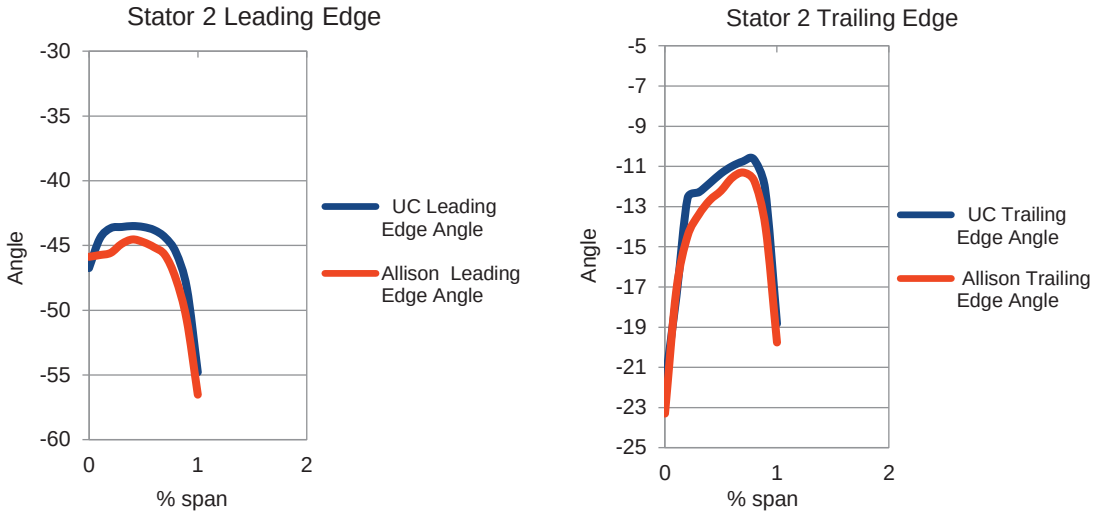

Figure 11.—Comparison of the trailing and leading edge of Stator 2.

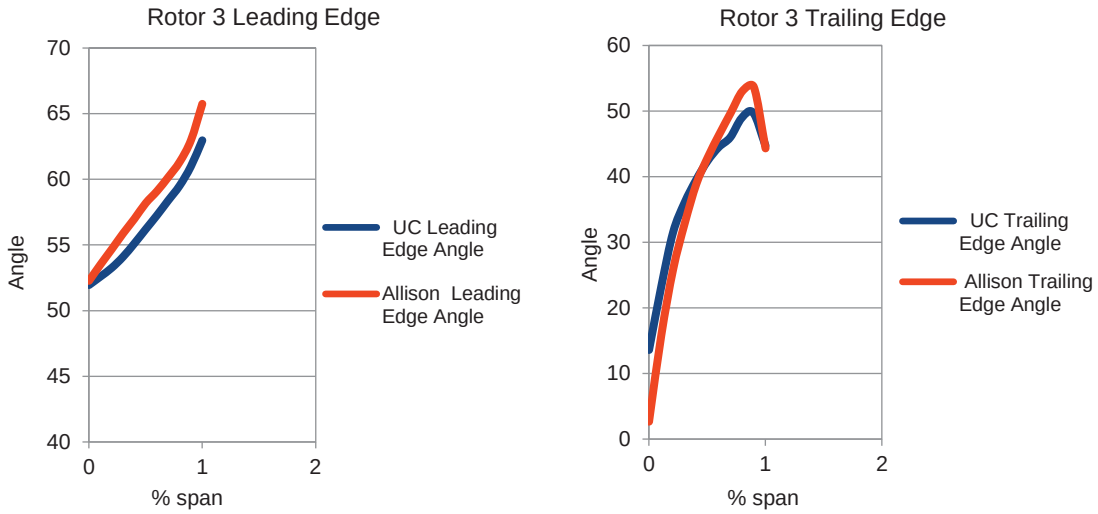

Figure 12.—Comparison of the trailing and leading edge of Rotor 3.

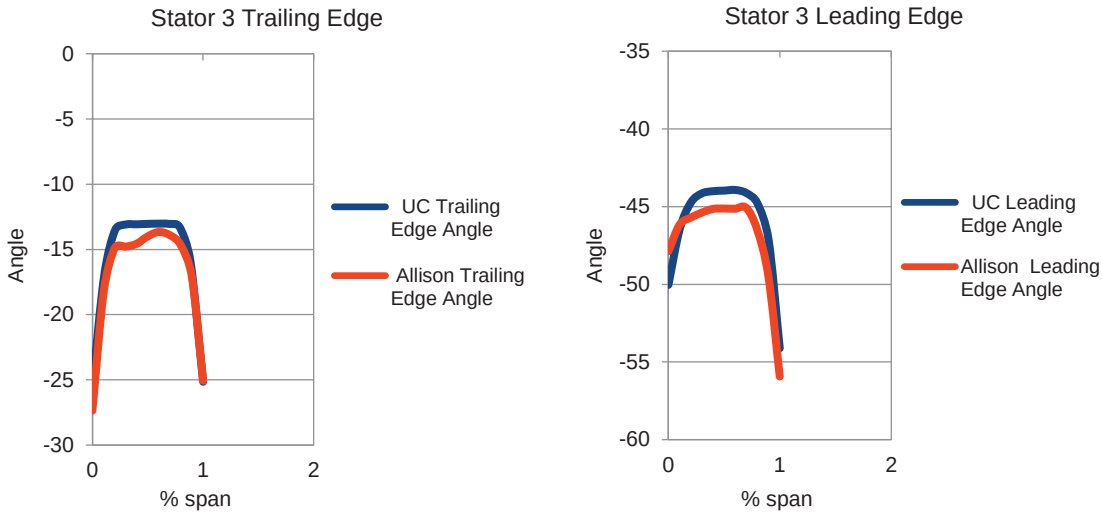

Figure 13.—Comparison of the trailing and leading edge of Stator 3.

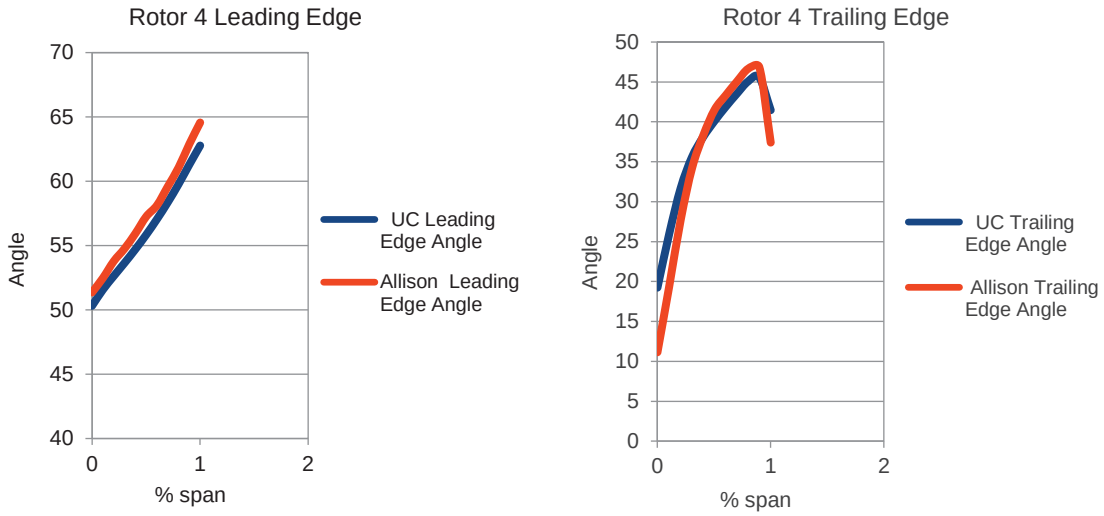

Figure 14.—Comparison of the trailing and leading edge of Rotor 4.

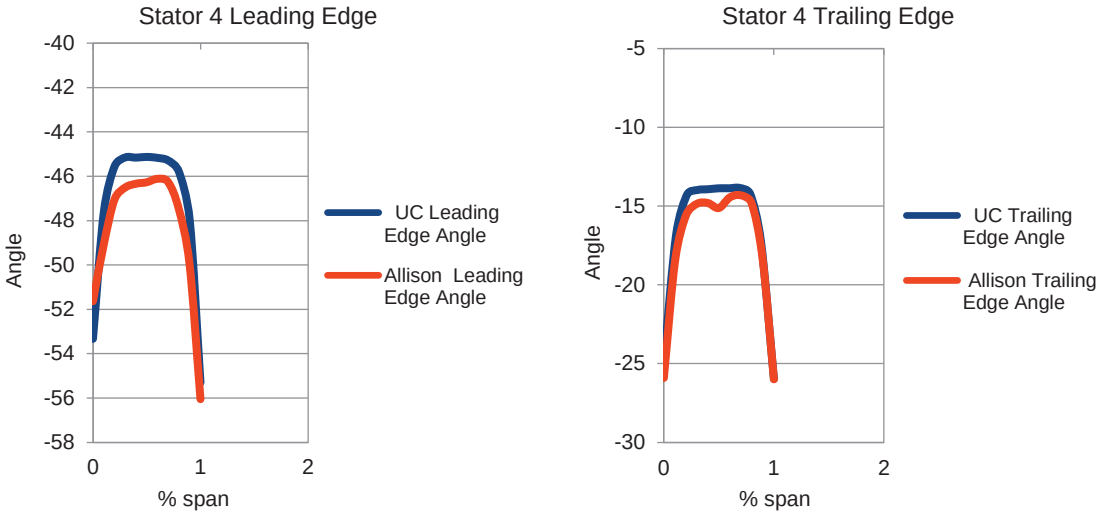

Figure 15.—Comparison of the trailing and leading edge of Rotor 4.

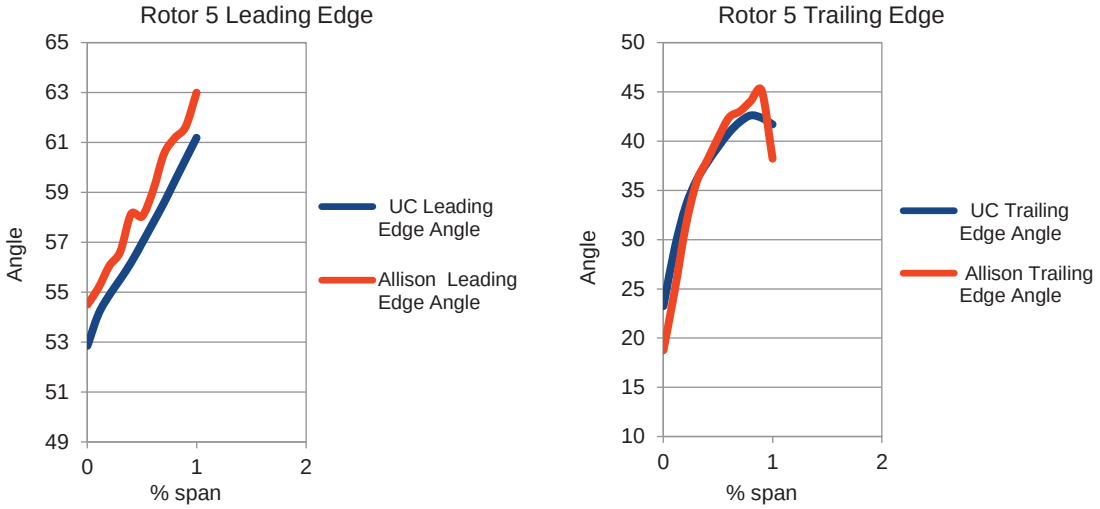

Figure 16.—Comparison of the trailing and leading edge of Rotor 5.

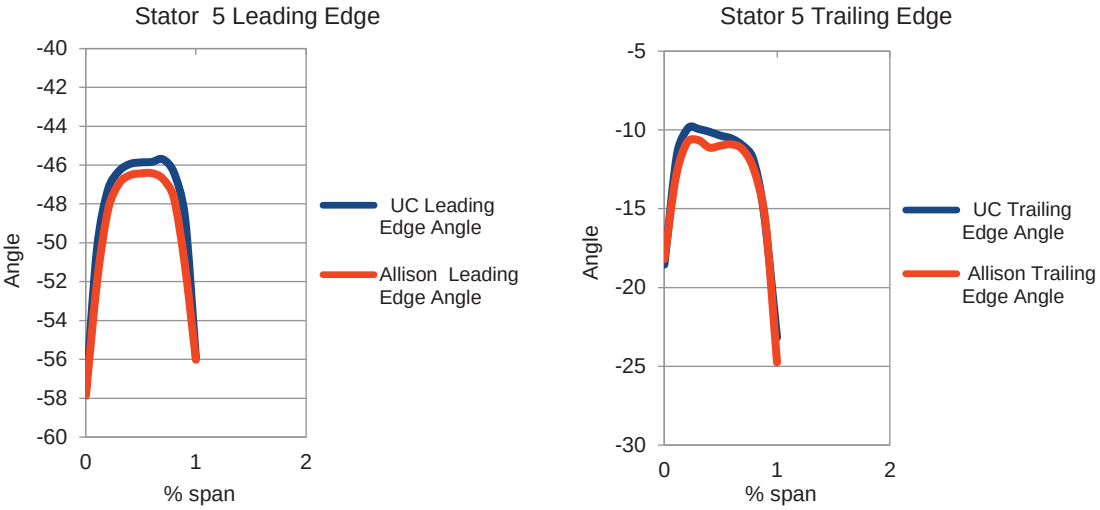

Figure 17.—Comparison of the trailing and leading edge of Stator 5.

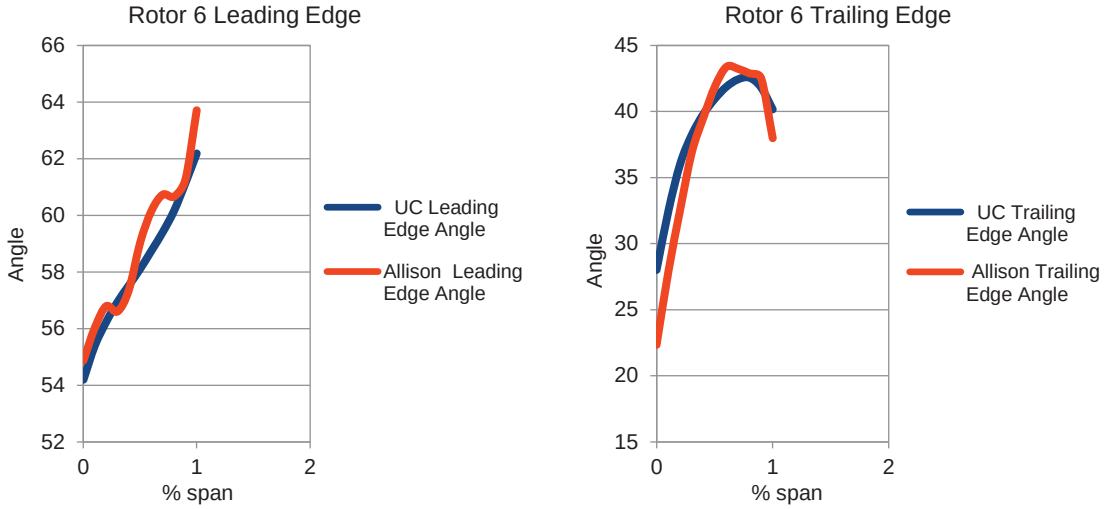

Figure 18.—Comparison of the trailing and leading edge of Rotor 6.

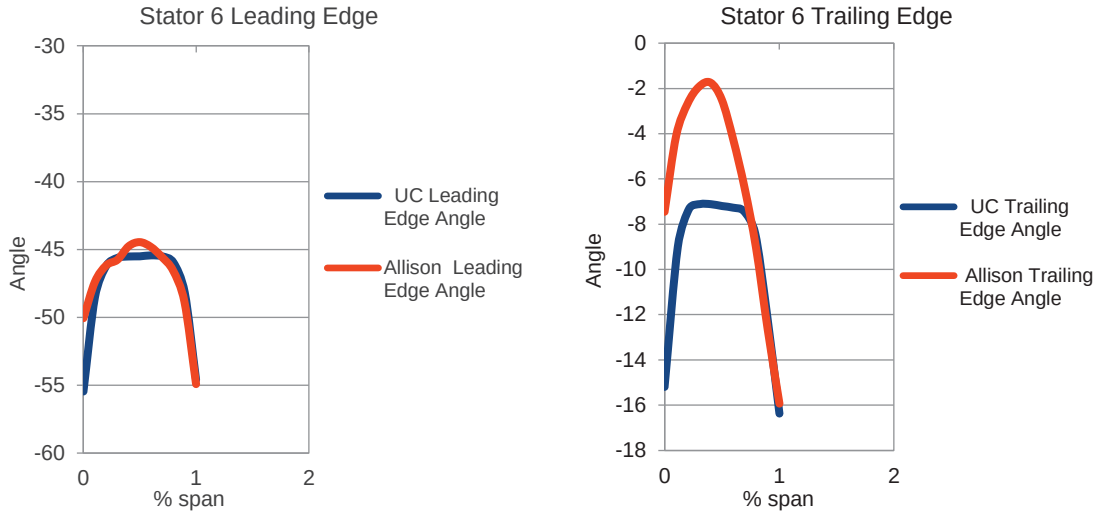

Figure 19.—Comparison of the trailing and leading edge of Stator 6.

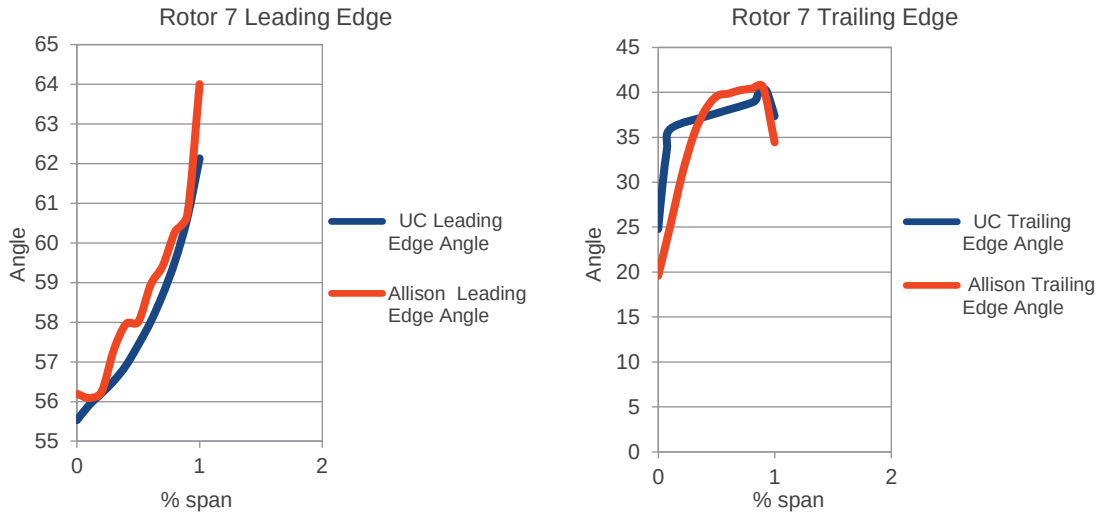

Figure 20.—Comparison of the trailing and leading edge of Rotor 7.

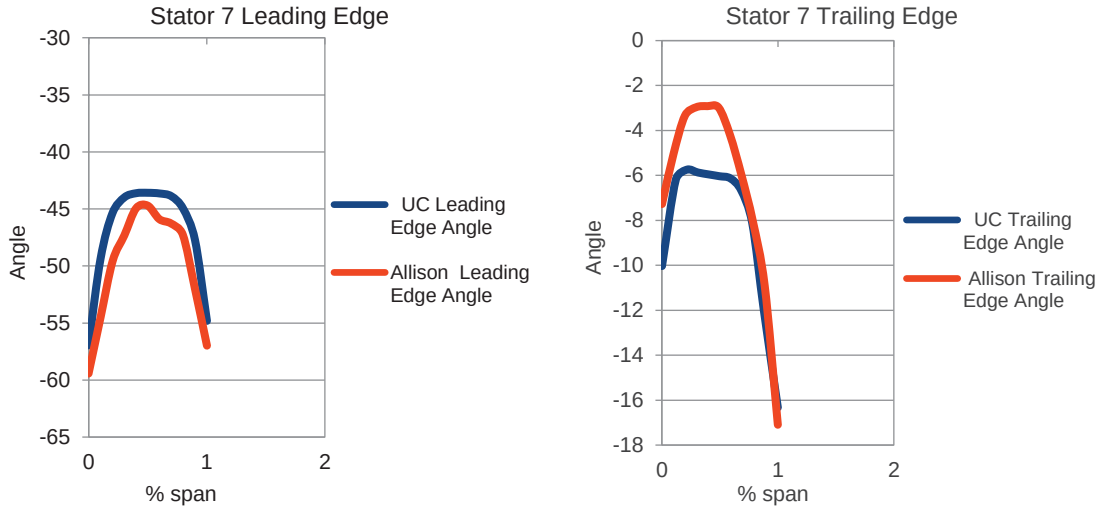

Figure 21.—Comparison of the trailing and leading edge of Stator 7.

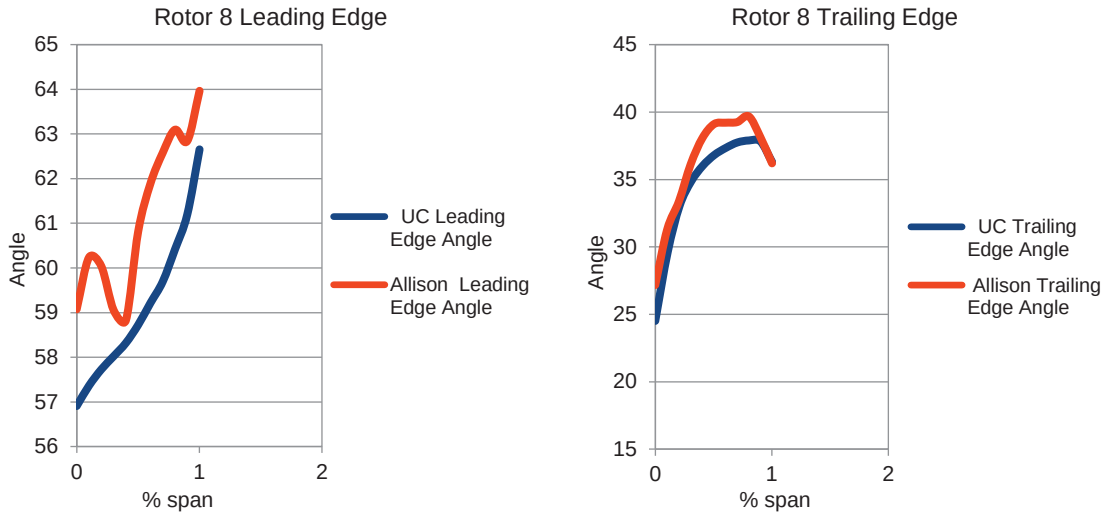

Figure 22.—Comparison of the trailing and leading edge of Rotor 8.

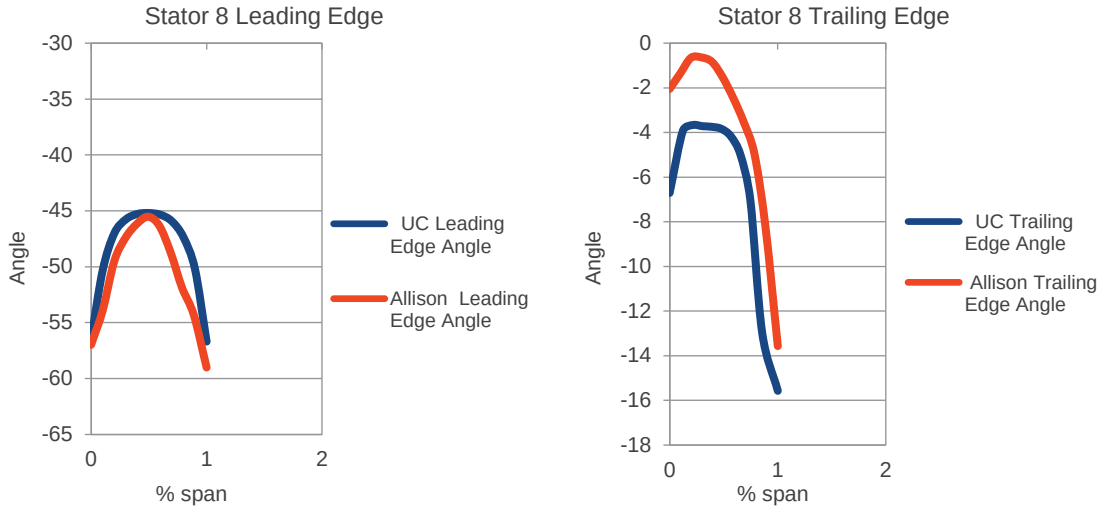

Figure 23.—Comparison of the trailing and leading edge of Stator 8.

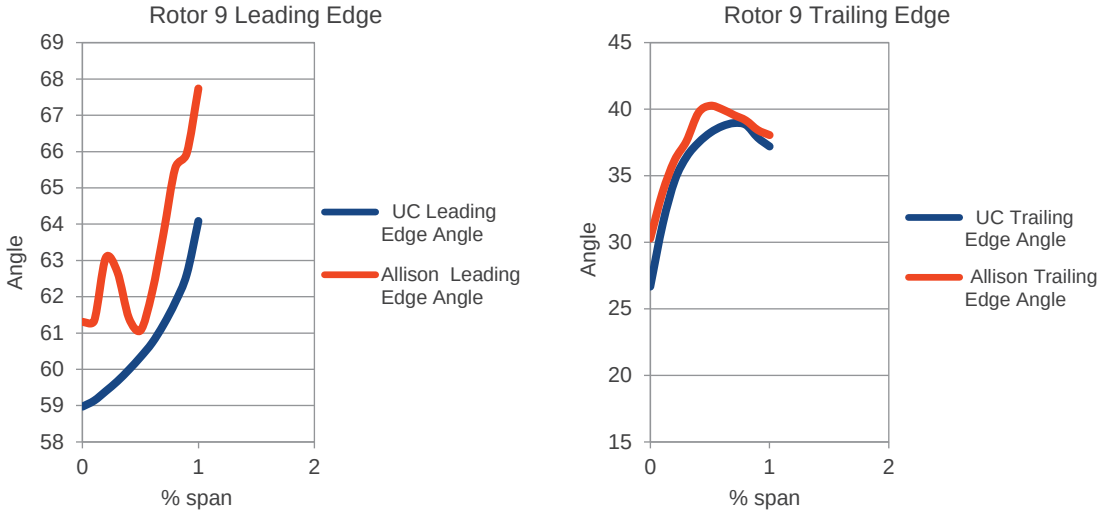

Figure 24.—Comparison of the trailing and leading edge of Rotor 9.

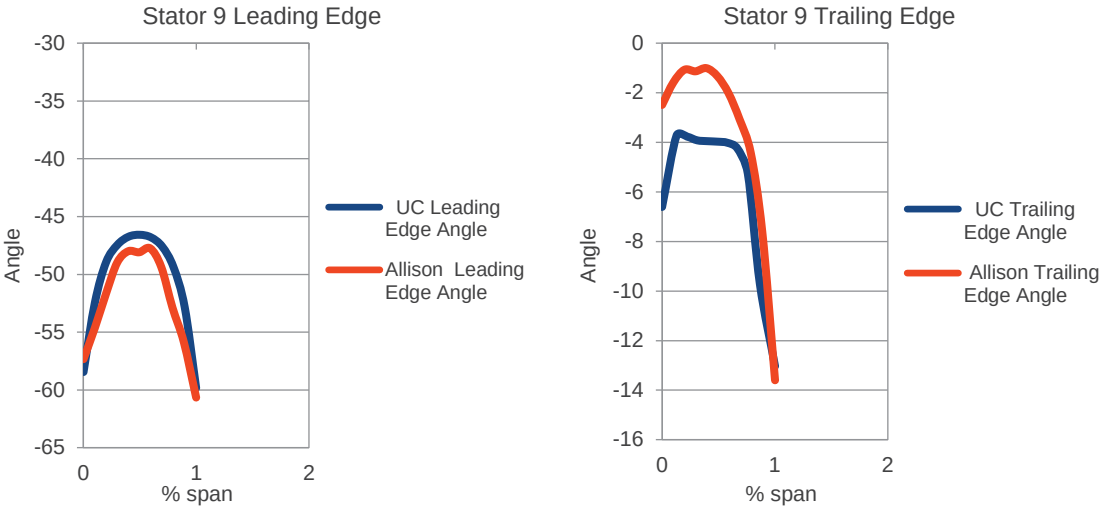

Figure 25.—Comparison of the trailing and leading edge of Stator 9.

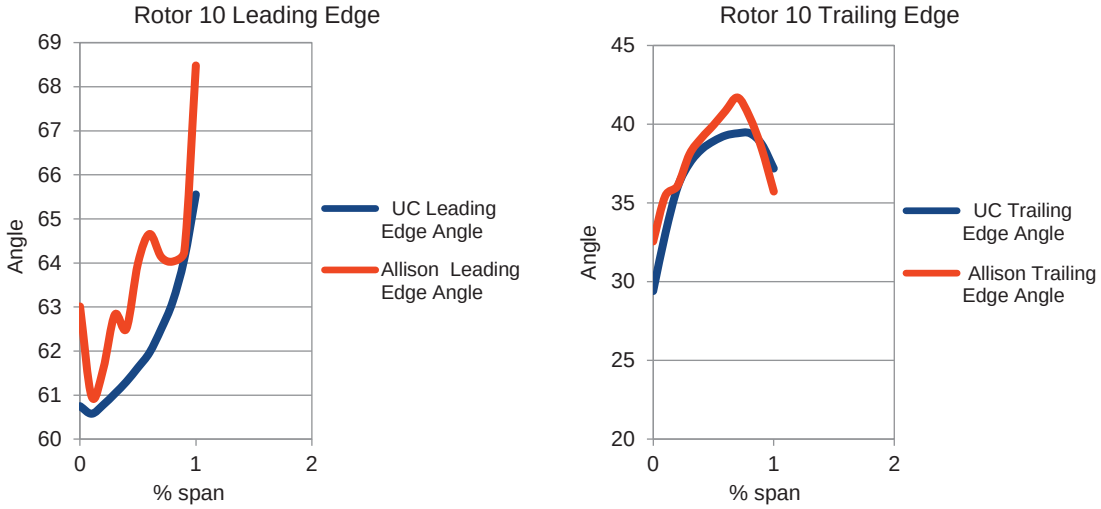

Figure 26.—Comparison of the trailing and leading edge of Rotor 10.

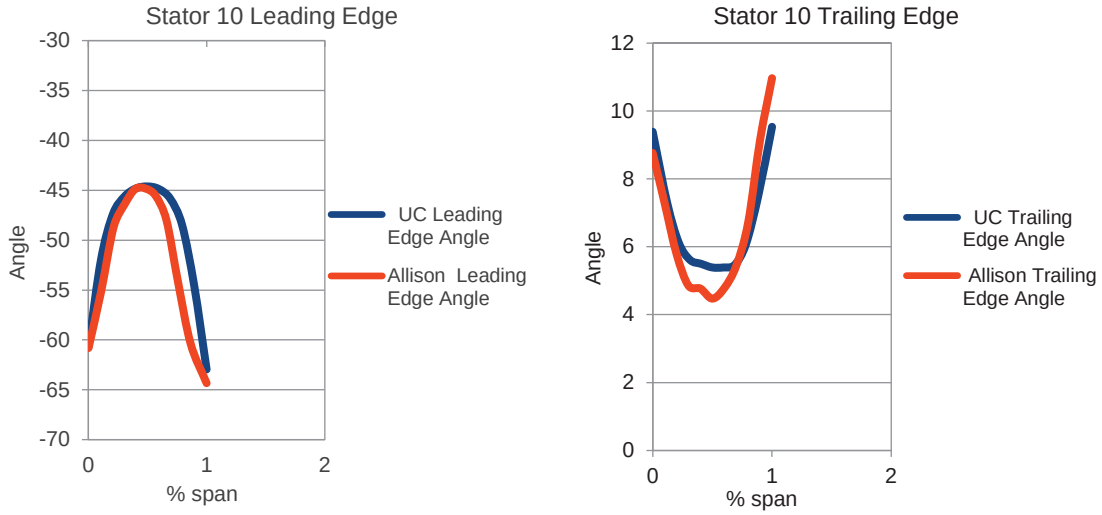

Figure 27.—Comparison of the trailing and leading edge of Stator 10.

References

1. Claus, R.W., Evans, A.L., Lytle, J.K., Nichols, L.D., "Numerical Propulsion System Simulation," Computing Systems in Engineering, Vol. 2, No. 4, pp. 357-364, 1991.
2. Claus, R.W., Townsend, S., "A Review of High Fidelity Gas Turbine Engine Simulations," ICAS 2010-475, Sept. 2010.
3. Turner, M.G., Reed, J.A., Ryder, R. and Veres, J.P., "Multi-Fidelity Simulation of a Turbofan Engine with Results Zoomed into Mini-Maps for a Zero-D Cycle Simulation," ASME Paper No. GT2004-53956, Vienna, Austria, June 2004 (also NASA/TM—2004-213076).
4. Hall, E., Owen, P., "Energy Efficient Engine HP/LP Spool Analysis," To Be Published.
5. Cline, S.J., Kutney, J.T., Halter, P.H., Sulivan, T.J., "Energy Efficient Engine Fan and Quarter-Stage Component Performance Report," NASA CR-168070, Jan. 1983.
6. Holloway, P.R., Knight, G.L., Koch, C.C., Shaffer, S.J., "Energy Efficient Engine High Pressure Compressor Detail Design Report," NASA CR-165558, May 1982.
7. Timko, L.P., " Energy Efficient Engine High Pressure Turbine Component Test Performance Report," NASA CR-168289.
8. Hall, E., Delaney, R., Lynn, S., and Veres, J. "Energy Efficient Engine Low Pressure Subsystem Aerodynamic Analysis," NASA/TM—1998-208402.
9. Hall, E., "Modular Multi-Fidelity Simulation Methodology for Multiple Spool Turbofan Engines," NASA High Performance Computing and Communications Computational Aerosciences Workshop, NASA Ames Research Center, February 15-17, 2000.
10. Stearns, EM, et al, "Energy Efficient Engine Integrated Core/Low Spool Design and Performance Report," NASA CR-168211, 1985.
11. Bridgeman, M.J., Cherry, D.G., Pedersen, J., "NASA /GE Energy Efficient Engine Low Pressure Turbine Scaled Test Vehicle Performance Test," NASA CR-168290, July 1983.
12. Vilmin, S., Lorrain, E., Hirsch, CH., Swoboda, M., "Unsteady Flow Modeling Across the Rotor / Stator Interface Using the Nonlinear Harmonic Method," ASME GT2006-90210.